

## Transports, frontal motions and eddies at the Brazil–Malvinas Currents Confluence

SILVIA L. GARZOLI\* and ZULEMA GARRAFFO†

(Received 3 April 1988; in revised form 10 October 1988; accepted 12 December 1988)

**Abstract**—Three inverted echo sounders were deployed to study the dynamics of the western South Atlantic Brazil–Malvinas Confluence region. From the original travel time data obtained with the sounders, the dynamic height of the surface relative to 800 m at the three locations was obtained and geostrophic velocities between sites calculated. The time-averaged geostrophic velocity of the Brazil Current (relative to 800 m) during the observed period is  $35 \text{ cm s}^{-1}$  ( $\pm 2.2 \text{ cm s}^{-1}$ ) and the mean transport relative to 800 m is 11 Sv. For the Malvinas Current return flow, the mean geostrophic velocity is  $9 \text{ cm s}^{-1}$  ( $\pm 2.0 \text{ cm s}^{-1}$ ) and the mean associated transport 3.5 Sv. Cold intrusions are observed in offshore records during the 17-month recorded period, some of them associated with cold cyclonic eddies with available potential energy of  $6.3 \times 10^{15} \text{ J}$ . Using a simple model the location of the thermal front is obtained from the time series of the depth of the thermocline. Results show that the main motion of the front is an east–west displacement for distances of about 100 km; the observed period occurs with a periodicity of 12 months and is related to a variability in the latitude of maximum northward penetration of the Malvinas Current. Motions of the front, with a period of 1–2 months, are probably related to a north–south variation of the latitude of return of the Brazil Current.

### 1. INTRODUCTION

THE general circulation of the southwestern Atlantic, off Argentina, is characterized by the confluence of the cold north-flowing Malvinas Current and the warm south-flowing Brazil Current. The confluence originates near  $38^\circ\text{S}$ , creating a strong thermal front with gradients up to  $1^\circ\text{C}/250 \text{ m}$ . Satellite infra-red observations obtained during 1976–1979 (LEGECKIS and GORDON, 1982) show that the Brazil Current displays north–south fluctuations between  $38^\circ$  and  $46^\circ\text{S}$  with a time scale of about 2 months. Warm-core eddies are formed as a detachment of the southward extension of the Brazil Current; cold-core eddies also are observed though they form less frequently.

Recent studies in the area (RODEN, 1986; BROWN *et al.*, 1986; OLSEN *et al.*, 1986; GORDON, 1989; OLSON *et al.*, 1988) show the complexity of the dynamics at the confluence zone. From XBT/CTD casts, obtained during legs 7 and 8 of the *Marathon* cruise (CAMP *et al.*, 1985; RODEN and FREDERICKS, 1986), a composite figure of the topography of the area, as inferred from the depth of the  $8^\circ$  isotherm, was obtained by Roden (Fig. 1). The Brazil Current, here indicated where the depth of the  $8^\circ$  isotherm exceeds 500 m, flows southward to about  $43^\circ\text{S}$  and then meanders back toward subtropical latitudes. The meanders have a wavelength of 400–500 km and a wave amplitude of roughly 200 km (RODEN, 1986). Two large warm-core eddies occur in the vicinity of the

\* Lamont-Doherty Geological Observatory of Columbia University, Palisades, NY 10964, U.S.A.

† CIMA/CONICET, Arenales 1678, C1061 Buenos Aires, Argentina.

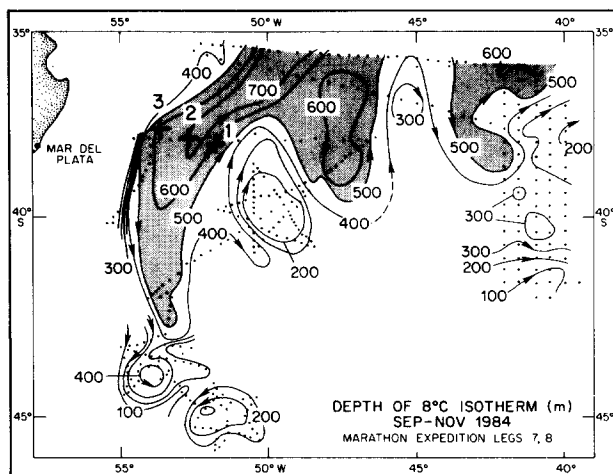


Fig. 1. Depth of 8° isotherm in the Argentine Basin during the austral spring of 1984, from RODEN (1986). The contours between 38°S–46°S and 46°W–56°W were kindly furnished by A. Gordon. Shading indicates Brazil Current water; arrows indicate the flow direction. The crosses indicate the locations of the sounders: IES Sta. 1, 37°58'S, 51°56'W; IES Sta. 2, 37°47'S, 52°46'W; IES Sta. 3, 37°29'S, 53°49'W.

Brazil Current return flow, near 45°S; a large cold-core eddy is centered at 39°S, 50°W (GORDON, 1989). The meander near 42°W appears to be near detachment to form a warm-core eddy.

As part of a multi-institutional study in this area, a small array of inverted echo sounders was deployed during November 1984 and maintained until the end of March 1986; locations are shown in Fig. 1. The objective of this preliminary experiment was to monitor the time-space variability of the confluence front and its relation with the meridional migration of the currents.

Two instruments were recovered and three redeployed in June 1985. The data collected during the first period of deployment (November 1984 to June 1985) at two locations (IES3 and IES1) were analysed by GARZOLI and CLEMENTS (1986) and GARZOLI and BIANCHI (1987). The observed travel times were calibrated for dynamic height from which geostrophic velocities can be inferred between the inverted echo sounder locations. In addition, a parameter that determines the position of the subsurface front was obtained.

The main results from this previous analysis can be summarized as follows: the time series of dynamic height at the offshore location indicates the presence of a cold intrusion during November 1984, the southward extension of the Brazil Current and the northward extension of the Malvinas Current during January 1985, and a simultaneous warming of the area at both locations (0.04 dyn m/month) from March to June. The mean value of the surface geostrophic velocity (relative to 800 m) is  $-14 \text{ cm s}^{-1}$ , equivalent to an average southward transport of  $10 \times 10^6 \text{ m}^3 \text{ s}^{-1}$  (10 Sv). The maximum calculated southward transport,  $23 \times 10^6 \text{ m}^3 \text{ s}^{-1}$ , is observed during January 1988. The front oscillates around its mean position with a period of about 1 month and an amplitude from 10 to 50 km. The velocity of the displacement achieves values up to  $10 \text{ km day}^{-1}$ .

In this paper, the results from the second period of recovery (June 1985 to March

1986), are presented and the complete 17 months time series discussed and analysed in terms of the local dynamics. Hydrographic data are combined with dynamic height time series to study the geostrophic velocities and transports associated with the Brazil and Malvinas currents at their confluence. From the time series of dynamic height and depth of the main thermocline, the low-frequency variability of the thermal front is analysed. Anomalies in dynamic height detected in the records are associated with cold and warm intrusions and cold cyclonic eddies; the surface velocity and the available potential energy for the eddies are estimated.

## 2. THE DATA

Three inverted echo sounders (IES) were deployed from the R.V. *Oca Balda* OB-0485) during June 1985 and recovered during March 1986 (cruise OB-0286). The location of the instruments, the depth of the deployments and the sampling period are given in Table 1 together with the location of the deployments during the first part of the experiment (GARZOLI and BIANCHI, 1987). During the cruise, CTD/XBT casts were obtained both to determine the characteristics of the water column along the line of deployments at the beginning and end of the time series as well as to calibrate the instruments.

In this section a brief description of the calibration of the data to standard parameters (e.g. dynamic height, depth of the thermocline and distance to the front) is presented. A more detailed explanation and justification of the calibration of the travel time series is given in GARZOLI and BIANCHI (1987). During the first period of deployment and due to the malfunction of one of the instruments, the sampling in time of the time series was reduced considerably (GARZOLI and BIANCHI, 1987). In this paper, for consistency with the first part, time series of dynamic height are shown as 10-day averages of the daily values. This is not the case for the time series of the distance to the front. Better resolution in time improves comparison with satellite images, for example, and 5-day averages of the daily values are presented.

### *Calibration to dynamic height*

Travel time has been demonstrated to vary linearly with dynamic height (WATTS and ROSSBY, 1977).

By definition travel time (TT) is a function of the sound velocity,  $c$ :

$$TT = -2 \int_b^s dz/c(T, S, P), \quad (1)$$

Table 1. Location of the moored instruments, depth of the deployment, sampled period and sampling interval

Station no./site	Latitude (S)	Longitude (W)	Depth (m)	First–last sample	$\Delta t$ (h)
IES 1	37°58.70'	51°56.40'	4351	11/09/84–06/20/85	0.5
IES 1	37°58.08'	51°56.37'	4350	06/20/85–03/24/86	1
IES 2	37°46.46'	52°45.52'	3803	06/19/85–03/23/86	1
IES 3	37°29.30'	53°49.30'	1096	11/09/84–06/19/85	0.5*
IES 3	37°28.91'	53°49.39'	1112	06/18/85–03/23/86	1

\* Original sampling, due to malfunction the final sampling was reduced to a block average of  $\Delta t = 2$  days.

where  $c$  is a direct function of the temperature ( $T$ ), salinity ( $S$ ), and the pressure ( $P$ ); the integral extends from the bottom ( $b$ ) to the surface ( $s$ ). Thus, travel time varies inversely with  $T$  and  $S$ . This variability in the water column can be related to upward (downward) motions of the main thermocline that result in variability of dynamic height and therefore in variability of the geostrophic shear of the currents. Given a CTD cast close to the bottom, it is possible to calculate the travel time and the dynamic height from the  $T$ ,  $S$ , and  $P$  values. By doing this for a substantial number of casts, an accurate correlation between the variables can be obtained.

This calibration was done using the method described in GARZOLI and BIANCHI (1987). In that paper the highest correlation was found between the bottom to surface travel time and dynamic height of the surface relative to 800 m, and it was shown that most of the variability occurs in the upper layer, which implies the dominance of the baroclinic setup. The result was confirmed by GORDON (1989), who found that the high correlation between the depth of any mid-thermocline isotherm and the 0/1500 dynamic height anomaly is essentially an expression of the dominance of the thermocline baroclinicity over that of the deeper water.

New values, from the CTD cast obtained during the last cruise, were added to the regression curve between the two variables. They fit into the regression, change the values of the constant of proportionality only in order of  $10^{-4} \text{ m ms}^{-1}$ , and increase the precision. The relation between relative changes in travel time and relative changes in dynamic height, is given by

$$\Delta DH(\text{dyn m}) = -0.01576 \Delta TT(\text{ms}). \quad (2)$$

The coefficient of determination of the regression is  $r^2 = 0.98$  and the error of the estimate,  $\pm 0.0206 \text{ dyn m}$ .

Time series of relative dynamic height are calculated from the observed relative travel time using relation (2). The absolute value of dynamic height was then estimated by adjusting the beginning and the end of the records to dynamic height values obtained with data from a CTD cast at the location of the instrument after deployment and before recovery. Two criteria are used when following this procedure: minimize the error at both edges and minimize the error in geostrophic velocity between stations. The last procedure was done by calculating the geostrophic velocity from the difference in dynamic height as obtained from the inverted echo sounder data and geostrophic velocities calculated from the two CTD casts at the deployment locations. The error incurred using these procedures to obtain the absolute dynamic height ranges from 0.005 to 0.01 dyn m.

With the calibration method described in this section, the dynamic height time series has an error of less than  $\pm 0.03 \text{ dyn m}$ . The error in the calculation of geostrophic velocities varies from  $\pm 1.35$  to  $\pm 2.25 \text{ cm s}^{-1}$  depending on the time series used to obtain the difference in dynamic height.

The time series of dynamic height of the surface relative to 800 m obtained at the three locations during the second part of the experiment (Table 1) are shown in Fig. 2. The circles ( $\oplus$ ) at the edges represent the dynamic height values calculated from the hydrographic observations. The gap between the CTD and inverted echo sounder values at the beginning of IES Sta. 1 (MIL) is due to the fact that the instrument collected data for a period of 2 days, then stopped recording the data, and started working again 10 days later.

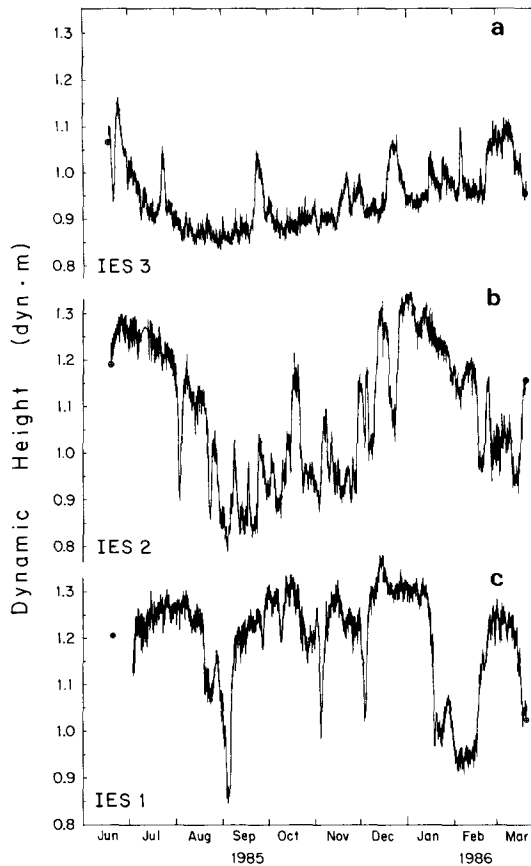


Fig. 2. Time series of dynamic height of the surface relative to 800 m at the three monitored locations of Table 1 during the period June 1985 to March 1986. The circles ( $\oplus$ ) at the edge are the values of dynamic height calculated from the hydrographic observations.

#### *Calibration of distance from the moored instruments to the thermal front*

As shown in GARZOLI and BIANCHI (1987) the vertical thermal structure of the region changes drastically with the position of the front. The presence of the Malvinas Current is represented by an almost homogeneous layer of colder water while the Brazil Current is associated to a sharp thermocline located at approximately 500 m depth. The currents meet, creating a long strong thermal front with a marked expression in the temperature field. The northward migration of the Malvinas Current results in an eastward motion of the surface front, while a westward displacement results from a southernmost penetration of the Brazil Current. Therefore if the depth of the main thermocline is known and a relation can be established between this depth and the position of the front, the east–west motion of the frontal zone can be studied. This is valid if the front executes this motion as a rigid body. The analysis of all available hydrographic data near 38°S (not shown) (see below) allowed us to conclude that this hypothesis is a good first approximation.

From the travel time series it is possible to determine the location of the main thermocline. If the depth of the thermocline is accurately represented by a specific isotherm, hydrographic stations can be used to determine, as was done with the dynamic

height, the relation between the variability in the depth of the isotherm and the travel time. GARZOLI and BIANCHI (1987) used the depth of the 10°C isotherm ( $z_{10}$ ) as an indicator of the main thermocline and established that the relation is linear, that both variables are highly correlated ( $r^2 = 0.99$ ), and that the ratio between  $z_{10}$  and travel time is  $-26.4 \text{ m ms}^{-1}$ . The required relation between  $z_{10}$  and the position of the front is given by a polynomial fit to the observed data. Due to the extremely weak slope of the 10°C isotherm when it is more than 15 km westward of the sharp baroclinic front, values obtained more than 15 km west of the front are uncertain (GARZOLI and BIANCHI, 1987).

During the first period of the deployment (November 1984 to June 1985) the front was located either at, or west of, the inshore location (IES 3, EDU). From June 1985 to March 1986 the front was located mostly in an area where the extremely weak slope of the 10°C isotherm (about 100 km east of IES 3) did not allow the use of the previous calibration. Therefore it was decided to use the data provided by the sounder deployed at the intermediate location, 100 km east of the inshore IES, to determine the position of the front. But even at this easternmost frontal location, IES 2,  $z_{10}$  surfaces for short periods of time during the recorded period did not allow the determination of the frontal position.

The procedure adopted was to choose the depth of the 8°C isotherm ( $z_8$ ) to represent the main thermocline. A whole new calibration was done following the same procedure as for  $z_{10}$  and was applied to the time series. That the choice of  $z_8$  is as good as the choice of  $z_{10}$  to represent the thermocline is confirmed by the results of GORDON (1989): the relationship of the 8°C isotherm depth (or any mid-thermocline isotherm) to the dynamic height anomaly is linear, with a coefficient of correlation of 0.98, with 81% of the data points falling within 0.05 dyn m of the straight line fit value.

The linear relation between the depth of the 8°C isotherm and travel time as determined from the hydrographic casts is

$$\Delta z_8 = -19.9278 \Delta TT \quad (3)$$

with a correlation coefficient of  $r^2 = 0.99$  and an error of the estimate of  $\pm 16.5 \text{ m}$ . It was obtained by using the same sets of data from which the relation between TT and DH was derived.

A mean profile for  $z_8$  as a function of distance in the direction perpendicular to the shore was obtained by a composite of vertical sections constructed from data obtained by GUERRERO *et al.* (1986, 1987) and additional sections obtained from historical data. By definition, the front is at the location of the sounder ( $X = 0$ ) when the depth of the thermocline, represented by  $z_8$ , is 200 m.

The best fit for the distance to the front as a function of  $z_8$  (Fig. 3) was obtained as 4th degree polynomial in  $z_8$  for  $z_8 < 440 \text{ m}$ , and as a rational function of the form  $a(z_8 + b)^{-1}$  for  $z_8 > 440 \text{ m}$ . The coefficient of correlation for distances to the front of  $-20 < X < 20 \text{ km}$  ( $40 \text{ m} < z_8 < 440 \text{ m}$ ) is  $r = 0.95$ , with an error of the estimate for the distance of  $\pm 4.2 \text{ km}$ . For  $20 \text{ km} < X < 100 \text{ km}$  ( $z_8 > 440 \text{ m}$ ),  $r = 0.71$ , and the mean error of the estimate of the distance is  $\pm 15 \text{ km}$ . For  $X < -20 \text{ km}$  (and for  $X > 100 \text{ km}$ ), the distance to the front cannot be determined by this method because the isotherm becomes almost horizontal at small (and large) depths and the errors are large.

The above-described method of calibration was applied to the time series obtained with the two sounders deployed in the frontal zone (IES 3 and IES 2). When  $z_8$ , the inshore (IES 3) location was smaller than 50 m (and therefore errors larger), data from IES 2

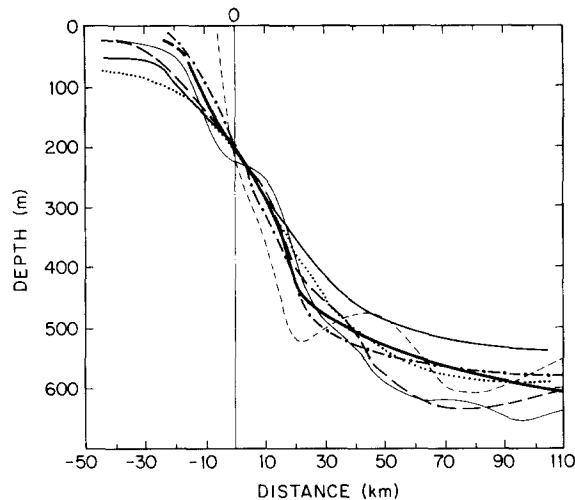


Fig. 3. Mean profile of the depth of the  $8^{\circ}$  isotherm in a section across the front as obtained from the best polynomial fit to hydrographic data. For simplicity, only six profiles used to obtain the fit are shown. Distances are measured relative to the western boundary of the front.

was used to estimate the position of the front. This was the case for the period July to December 1985. Results (Fig. 4) show the variability of the front with respect to the inshore location (i.e. when  $X = 0$  the front is located at IES 3), obtained as a composite of the distances observed from the time series of  $z_8$  obtained at IES Stas 3 and 2. Data were smoothed by a 5-day running mean average of the original values of  $z_8$  to eliminate the high-frequency present in the records. Positive distances indicate that the front is

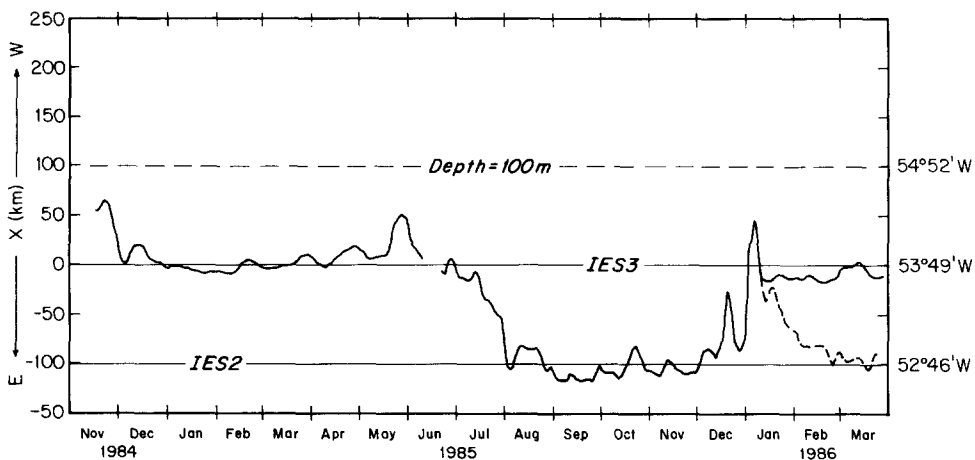


Fig. 4. Time series of the distance in kilometers from the front to the western location: (IES 3,  $37^{\circ}29'S$ ,  $53^{\circ}49'W$ ), for the 17 months of observation. Distance is positive when the front is located west of  $53^{\circ}49'W$ . As a continuation of the series obtained from the first deployment (GARZOLI and BIANCHI, 1987), a 5-day running average of the combined series is presented. The proximity to the coast is represented by the depth contour = 100 m.

located toward the west of IES 3 ( $53^{\circ}49'W$ ), and negative distances correspond to eastward movements with respect to this location. The gap in the data in June 1985 occurs where the time-series from the two deployments are connected: the averaging procedure results in a loss of data both at the end and the beginning of the series. By choosing the appropriate data set when the front is located at distances of more than 50 km, the error in the estimation of  $X$  in Fig. 4 has been kept lower than  $\pm 5$  km for almost the entire observed period.

An uncertainty in the front position occurs from 12 January, 1986, to the end of the record. Each instrument indicated a different position of the front (dashed line in Fig. 4). That the front was located near  $X = 0$  was decided on the basis of a simultaneous analysis of the dynamic height time series at the three locations, as will be discussed in Section 4.

### 3. GEOSTROPHIC VELOCITIES AND TRANSPORT

Three hydrographic sections, consisting of a combination of CTD and XBT casts, were obtained along the line of the moored instruments during the deployment and recovery cruises in November 1984, June 1985 and March 1986 (Fig. 5). Data from the two first sections (November 1984 and June 1985) were published and briefly described by GARZOLI and BIANCHI (1987) but they are included here in order to facilitate the discussion.

The variability of the vertical structure becomes evident when comparing the three sections. During mid-November 1984 (Fig. 5a) the front is located west of IES 3, and a cold intrusion appears at the location of IES 1. At the end of June 1985 (Fig. 5b), the front is located on top of the inshore instrument and the main core of the Milvinas Current has been displaced towards the east. The March section shows what we believe is a typical end-of-summer situation (Fig. 5c): the thermocline front is masked at the surface by summer warming of the sea-surface temperature which produces a shallow thermocline. A less pronounced temperature gradient, also generated at the surface, is observed approximately 40 km west of the subsurface front. It is interesting to note the existence of the two gradients in particular when considering satellite results. The sea-surface temperature, as revealed by the satellites, will detect a less intense thermal front located some tens of kilometers from the subsurface temperature and salinity front. This latter establishes the real division between the cold, fresh subantarctic water and the warm, saline Brazil Current.

The hydrographic sections (Fig. 5) show the conditions of the water column at the beginning, in the middle and at the end of the time series obtained with the inverted echo sounders. The CTD casts obtained at the locations of the deployed instruments were used to calibrate the travel time series to dynamic height values. Therefore results obtained at the beginning and at the end of the series should agree, within the limits of errors, with those derived from the hydrographic observations.

In what follows, the geostrophic velocities between stations and transport (relative to 800 m) as obtained from the CTD data are presented. The variability in time or how the system evolves from one state to the other (Fig. 5, top to bottom) will be discussed from the dynamic height time series obtained with the IES.

#### *From CTD data*

Geostrophic velocities and transport relative to 800 m were calculated from the CTD casts across the three zonal sections (Figs 5 and 6). This level of reference was chosen for



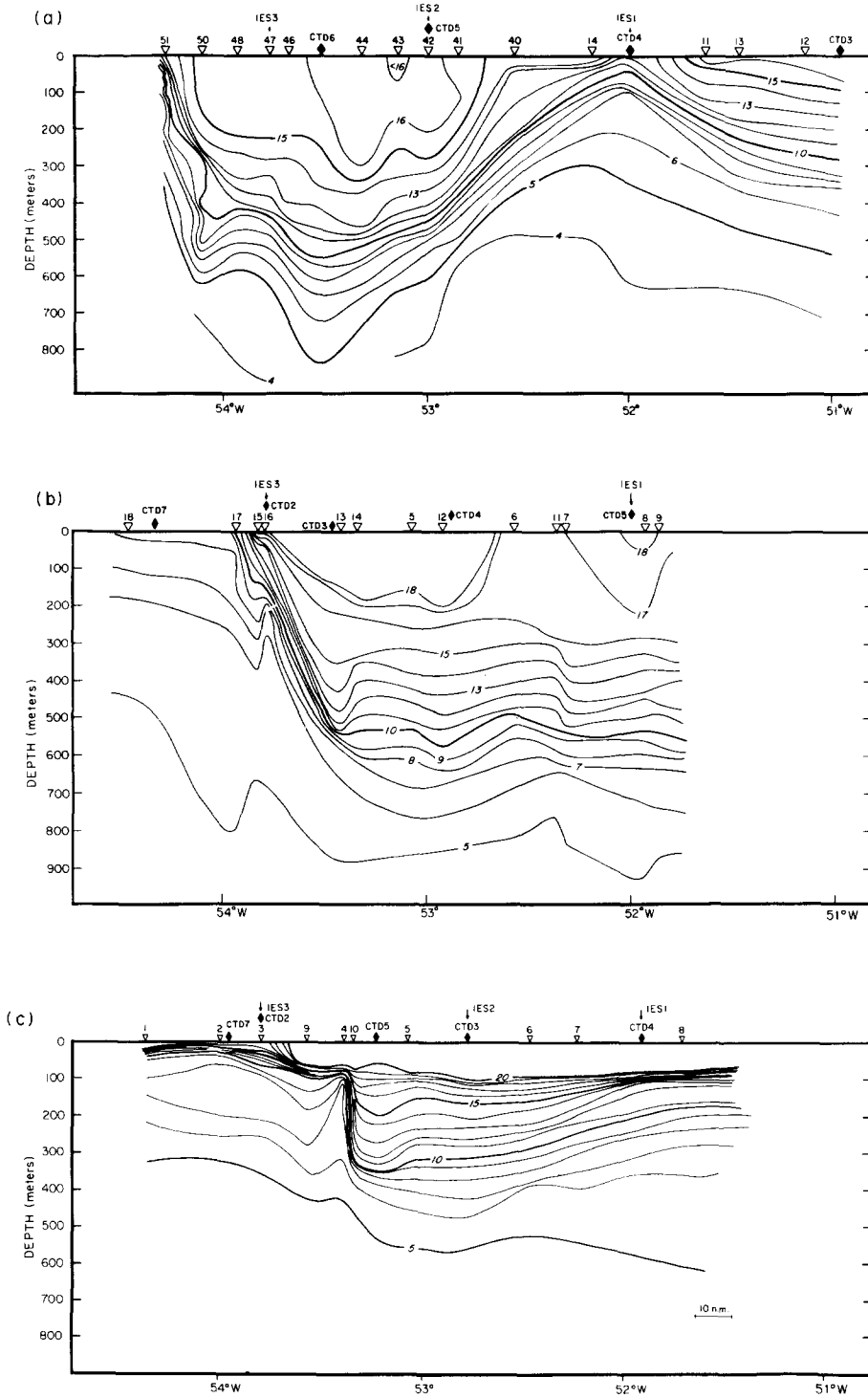
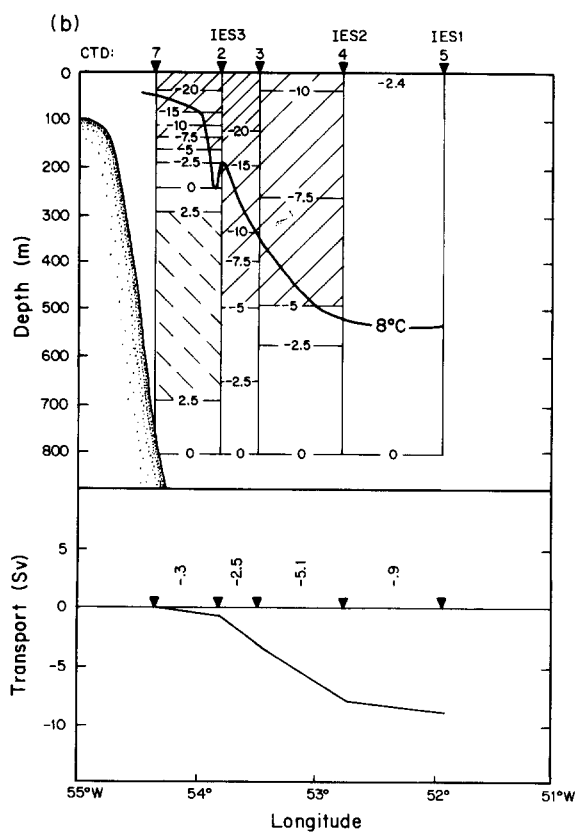
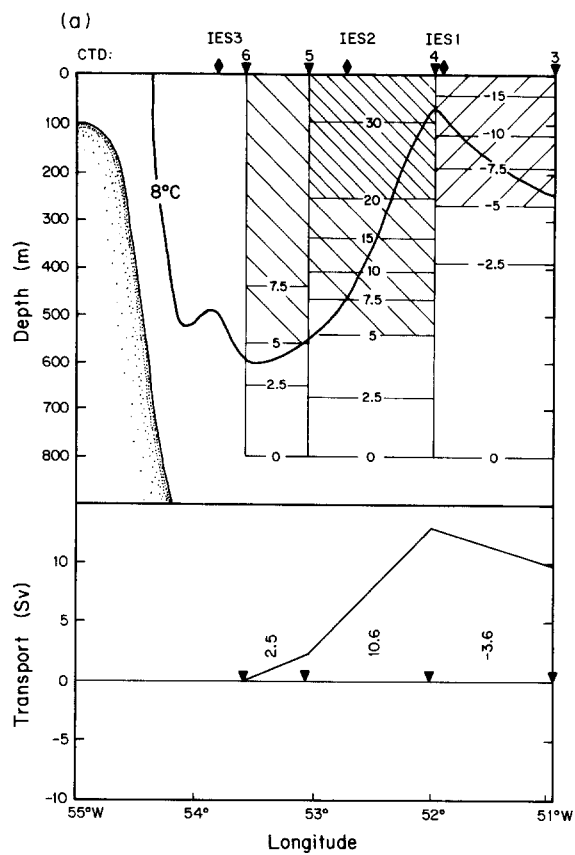


Fig. 5. Vertical temperature sections of transects during (a) 7–12 November 1984, (b) 18–22 June 1985 (from GARZOLI and BIANCHI, 1987), and (c) 22–25 March 1986.



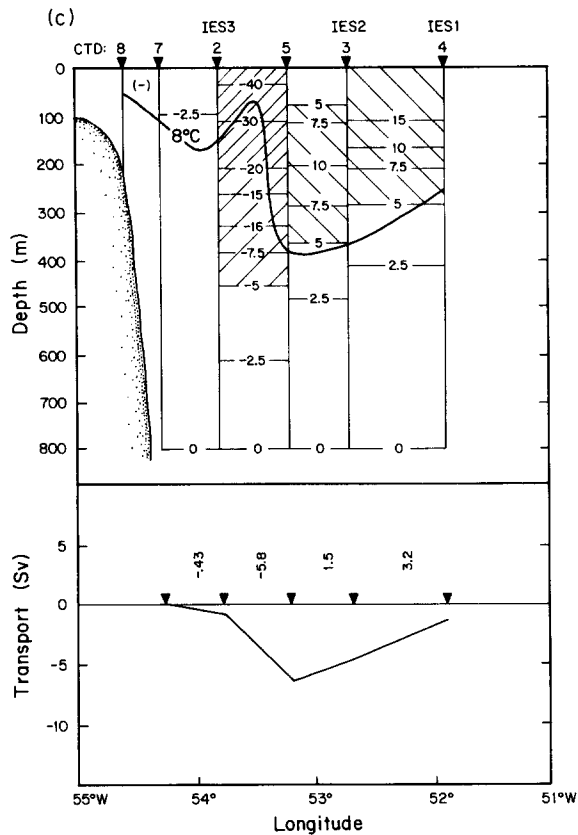


Fig. 6. (a) Geostrophic velocity ( $\text{cm s}^{-1}$ ) relative to 800 m (top) and accumulated transport (Sv) as obtained from the hydrographic stations. The symbols are: IES, IES station;  $\blacktriangledown$ , CTD station. The depth of the  $8^\circ\text{C}$  isotherm as obtained in Fig. 5, November 1984, is shown. (b) Same as (a) for June 1985. (c) Same as (a) for March 1986.

two reasons: (1) to compare with the results from the dynamic height time series obtained with the inverted echo sounders, noting that the highest degree of correlation is between the integrated measurement obtained with the instruments and the surface dynamic topography relative to 800 m (GARZOLI and BIANCHI, 1987); (2) to include in the calculation all available CTD stations, which in general were between 900 and 1500 m depth. In order to compare with previous calculations of transport in the area (GORDON and GREENGROVE, 1986), geostrophic velocities and transport relative to 1400 m were calculated at all stations that reached that depth. It is concluded that values relative to 800 m reach approximately 75% of values relative to 1400 m; this is in good agreement with the assumption that most of the flux occurs in the upper layer and with the choice of the 800 dbars reference level.

The November 1984 section (Fig. 6a) shows that between CTD Stas 6 and 4, the geostrophic flow is northward, while between CTD Stas 4 and 3 the current is toward the south. The northward surface velocity between CTD Stas 6 and 5 is  $9.4 \text{ cm s}^{-1}$ , and between CTD Stas 5 and 4, the surface velocity reaches the values of  $32.6 \text{ cm s}^{-1}$ . During

October, GORDON (1989) detected the presence of a cold eddy at the location of the easternmost deployment. Satellite images (OLSON, personal communication) show a consistent pool of cooled Brazil Current separated from the warm water to the north by a cold band of Malvinas flow. The gap between when images are available, 21 and 30 October and 17 and 22 November 1984, coincides with the period of the CTD observations, 7–13 November. The time series of dynamic height from the inverted echo sounders indicates during November the presence at the offshore location of a cold intrusion in a warm medium. Also, the difference in dynamic height between Stas 1 and 3 is positive, indicating northward flow. Therefore, we believe that at the time of the CTD observations a cold intrusion is present in the warm Brazil Current. Unfortunately, with only two points of observations we cannot determine the validity of this hypothesis. In any case, we are observing a cold intrusion with water characteristics corresponding to those of the Malvinas Current. We tend to believe that the southward velocities are associated with the component of cyclonic motion.

The winter situation observed during June 1985 (Fig. 6b) is different. According to Fig. 5, the front is located between XBT Stas 15 and 17 ( $53^{\circ}55'W$ ), that is to say, between CTD Stas 7 and 2. If we define the front as the position where the depth of the  $8^{\circ}C$  isotherm is 200 m, then the front would be located at CTD 2. These results are in coarse agreement with those from the satellite images. Between these two CTD stations (7 and 2), the surface velocity is negative ( $-20 \text{ cm s}^{-1}$ ), indicating southward motion. The observed flow is, for the reasons explained above, mostly due to the Malvinas return flow; the estimated transport is 0.3 Sv. East of CTD Sta. 2, negative (southward) velocities correspond to the Brazil Current and have a maximum value at the surface of  $28.3 \text{ cm s}^{-1}$  between CTD Stas 2 and 3. The total transport is  $-8.5 \text{ Sv}$ , which is again in good agreement with previously obtained values but possibly underestimated about 10% because the stronger velocities associated with the front are located west of CTD 2.

During March 1986 (Fig. 6c) the maximum surface velocity is observed:  $-45.4 \text{ cm s}^{-1}$  between CTD Stas 2 and 5. The depth of the  $8^{\circ}C$  isotherm, as derived from the combined CTD/XBT observations, shows that the front is located between these two stations at  $52^{\circ}20'W$ . Therefore, the observed flow is mostly due to the Malvinas return flow (0.4 Sv) but probably augmented by some component of the warm waters from Brazil. East of  $52^{\circ}20'W$  the southward transport (5.8 Sv) is due to the Brazil Current. This value is smaller than previous estimations and may be underestimated due to a northward flow on the western side of the front. The time series of dynamic height at the easternmost location (IES 1; Fig. 2) shows that starting in March 1986 the dynamic height decreases, indicating the formation of a cold eddy. XBT/CTD data (Fig. 5c) also show a shallowing of the isotherm east of  $53^{\circ}W$ . The infra-red images (not shown) for 26 March, 1986, show the presence of a cold eddy at the edge of the offshore location. We therefore conclude that the northward component of the velocities observed between CTD Stas 3 and 4 are due to a cyclonic motion originated by a cold eddy.

#### *Time variability from inverted echo sounder data*

The time dependence of the geostrophic velocities can be obtained from the dynamic height time series (Fig. 2). The surface geostrophic velocities relative to 800 m between pairs of stations (Fig. 7) were calculated from the 10-day running average time series of dynamic height using the relation:

$$v_g = g/f (\Delta DH / \Delta x), \quad (4)$$

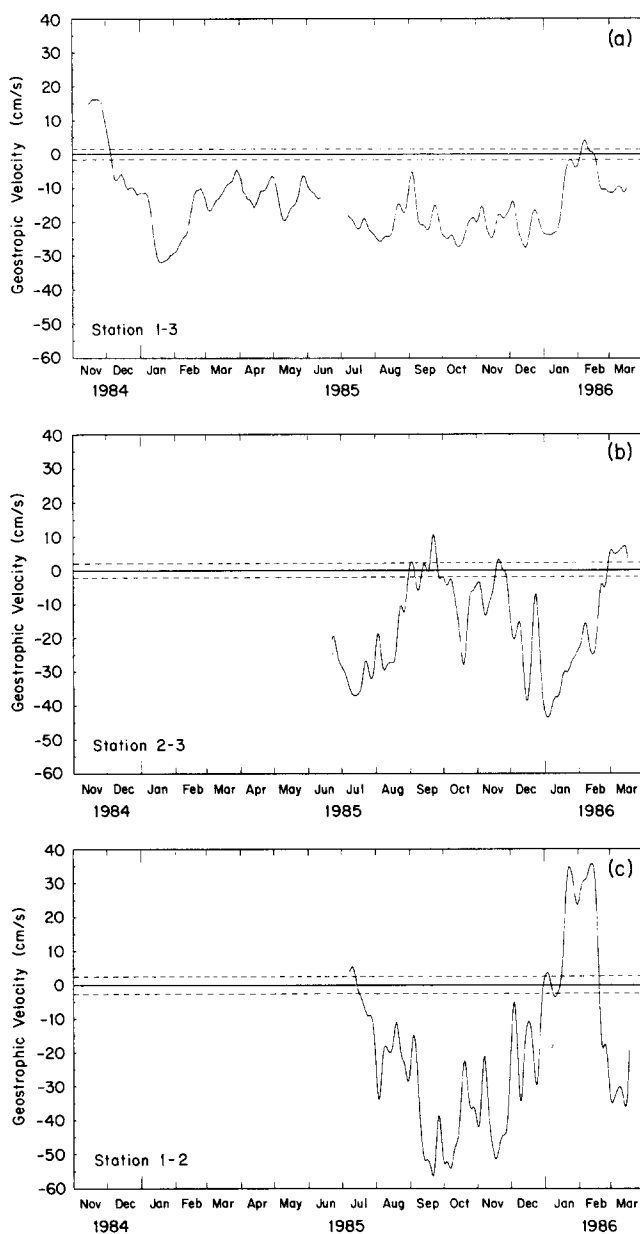


Fig. 7. Mean surface geostrophic velocity relative to 800 m normal to the line between pairs of IES stations, as a function of time during the total observed period. (a) Western and eastern locations; (b) western and intermediate locations; (c) intermediate and eastern locations. The dashed band around zero indicates the error bars.

where  $\Delta DH$  is the dynamic height difference between two stations separated by  $\Delta x$ ,  $g$  is gravity and  $f$  is the Coriolis parameter. The distance between stations is  $\Delta x = 102$  km for IES Stas 3 and 2, and  $\Delta x = 79$  km for IES Stas 2 and 1. The geostrophic velocities obtained between the westernmost and easternmost sites (IES Stas 3 and 1) also are included to compare the results with those from the first period of observation (Fig. 7a from November 1984 to June 1985).

From the geostrophic velocities, an estimate of the associated transport can be obtained. As the inverted echo sounder provides only an integrated quantity, it is necessary to assume that the velocity decreases linearly with depth. Figure 8 shows

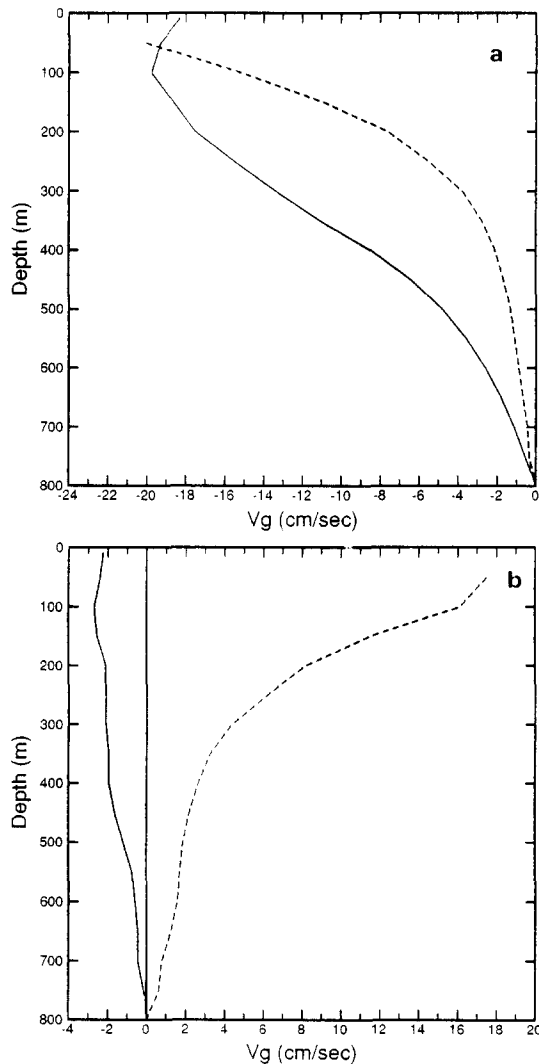


Fig. 8. Examples of vertical profiles of geostrophic velocities, reference 800 m. (a) From OB-0485, CTD Stas 4 and 2 (at IES 2 and 3) (solid line) and OB-0286 (dashed line) CTD Stas 3 and 2 (IES 2 and 3). (b) From OB-0485, CTD Stas 5 and 4 (at IES 1 and 2) (solid line) and OB-0286 (dashed line) CTD Stas 4 and 3 (at IES 1 and 2).

examples of the vertical profile of geostrophic velocities obtained from CDT stations obtained at the locations of the sounders. They represent one of the best (OB-85, Stas 5 and 4) and one of the worst cases (OB-86, Stas 3 and 2) for the approximation. In the first case, the difference between the two calculations for the transport is  $-0.2$  Sv; in the second case,  $4.6$  Sv. Calculations from all the available CTD stations for the transport between the surface to  $800$  m (not shown), using the exact and approximate method, determine that the errors range from  $-0.2$  to  $+4.6$  Sv, with a mean value for the difference of  $1.8$  Sv. Therefore, all values of transport obtained in the following section from the echo sounder data, should be considered only as an estimate.

During November 1984, the main flow between IES Stas 1 and 3 is towards the north (Fig. 7a). The geostrophic velocity reaches a maximum value of  $18 \text{ cm s}^{-1}$  and is associated with the cold intrusion observed in the hydrographic data (Fig. 6a). The northward motion calculated from the CTD casts is  $19.7 \text{ cm s}^{-1}$ . This reinforces our belief that we are observing a cyclonic motion. The maximum southward velocity of  $35 \text{ cm s}^{-1}$ , observed during January 1985, is related to a southward penetration of the Brazil Current waters (GARZOLI and BIANCHI, 1987).

After the passage of the cold intrusion, with the exception of a short period early in 1986, the main flow between IES Stas 1 and 3 is toward the south. The mean position of the front from January to April 1985 is  $X = 0$  km (Fig. 4, the front is at the location of IES Sta. 3). The mean geostrophic velocity between IES Stas 1 and 3 for that period of time is  $-16 \text{ cm s}^{-1}$ . Assuming that the velocity decreases linearly with depth from  $0$  to  $800$  m, the mean southward transport between these two stations is  $11.7$  Sv, which can be associated to the Brazil Current. The main geostrophic velocity increases from March to December 1985, from a mean monthly value of  $-10$  to  $-22 \text{ cm s}^{-1}$ . This is due to the eastward displacement of the thermal front; as can be seen in Fig. 4, the front located near  $X = 0$  km on March 1985, has moved by August 1985 eastward to a mean position  $X = -91$  km. The observed flow after August between these two stations (Fig. 7a) is therefore a composite of the southward flow associated with the Malvinas return flow and the Brazil Current. The monthly maximum southward transport for the composite flow is observed in December 1985, with a value of  $16 \times 10^6 \text{ m}^3 \text{ s}^{-1}$ .

A better zonal resolution is obtained for surface geostrophic velocities from June 1985 to March 1986. Figure 7b and c show the surface geostrophic velocities calculated between Stas IES 3 and 2 and IES 2 and IES 1, respectively. From June to August, a southward flow that reaches values of  $-37 \text{ cm s}^{-1}$  (Fig. 7b) is observed between IES Stas 3 and 2. Further east (Fig. 7c), the velocities are almost zero for June and increase to  $-30 \text{ cm s}^{-1}$  in August. This corresponds to a situation in which the front moves from west to east (Fig. 4).

From August to November 1985, the mean value of the position of the front is  $X = -103$  km, near IES Sta. 2 (Fig. 4). In this situation, the mean southward flow observed between IES Stas 3 and 2 (Fig. 7b) will correspond to the Malvinas return flow, while between Stas 2 and 1 (Fig. 7c) the flow corresponds to the Brazil Current. During this period the mean surface geostrophic velocity associated with the Malvinas return flow is  $-8.7 \text{ cm s}^{-1}$ , and the corresponding estimated transport is  $3.5$  Sv. The surface velocity associated with the Brazil Current is observed between IES Stas 2 and 1 (Fig. 7c), with a value of  $-35 \text{ cm s}^{-1}$  and transport of  $-11$  Sv. During September 1985 the mean position of the front is  $X = -113$  km ( $12$  km to the east of IES Sta. 2); maximum values of velocities are observed:  $-55 \text{ cm s}^{-1}$  at the surface between IES Stas 2 and 1 (Fig. 7c). This

Table 2. Values of transport as determined from the hydrographic data and estimated from inverted echo sounders observations

Flow	Brazil Current (Sv)	Malvinas return (Sv)
CTD, Nov. 1984	–	–
CTD, June 1985	–8.5	–0.3
CTD, March 1986	5.8	0.4
IES, Jan.–Apr. 1985	–11.7	–
IES, Aug.–Nov. 1985	–11.0	–3.5
IES, Oct. 1985	–11.0	–4.0

maximum southward flow is associated with the front, a result of part of the Malvinas return flow and the southward-flowing Brazil Current. The corresponding maximum southward transport for this composite flow is 18 Sv. The near-zero velocities observed between Stas 3 and 2 during September 1986 (Fig. 7b) could be explained as a cancellation of the northward flow of Malvinas and part of its return.

The northward velocities observed during mid-January and February 1986 (Fig. 7c) are associated with a cyclonic motion whose northward component reaches surface velocities of  $35 \text{ cm s}^{-1}$ . The main results described in this section are summarized in Table 2.

#### 4. FRONTAL MOTIONS AND EDDIES

The time series of dynamic height at the three moored locations (Table 1) and for the whole observed period (Fig. 9) have been smoothed by a 10-day running average of the original hourly values. The variability in dynamic height at the two westernmost locations (Fig. 9a,b, IES Stas 3 and 2) show different characteristics than the variability in dynamic height at the offshore location (Fig. 9c, IES Sta. 1).

The sharp front between the Malvinas and Brazil currents is generally located between the two westernmost moored locations (Fig. 4, November 1984 to July 1985, and December 1985 to March 1986). These sites are characterized by motions and oscillations of periods that range from 1 to 12 months. At the offshore location, generally in the core of the Brazil Current or its western boundary, the dynamic height is characterized by a rather constant value (1.25 dyn m), and sporadic cold (low) or warm (high dynamic height) anomalies that persist for periods of 10–40 days. These anomalies correspond to eddies or intrusions which are part of a more complex system associated with the poleward extension of the Brazil Current (LEGECKIS and GORDON, 1982). In this section these low-frequency motions and anomalies in dynamic height are derived from the position of the front (Fig. 4), the surface geostrophic velocity (Fig. 7) and the dynamic height variability (Fig. 8) calculated from those data.

##### *Frontal motions*

The frontal motions at  $38^\circ\text{S}$  are analysed on the basis of the position of the front derived from the depth of the thermocline (Fig. 4) and from the dynamic height time series at the westernmost locations (Fig. 8 top and middle panel). According to Fig. 4, the mean position of the front from December 1984 to May 1985 ( $\approx 6$  months) fluctuates around  $X = 0$ . From July to December similar fluctuations occur around a mean position displaced 100 km to the east ( $X = -103 \text{ km}$ ). After 6 months the front returns to  $X = 0$ . This low-frequency 100 km step motion is preceded in both cases by a fast east–



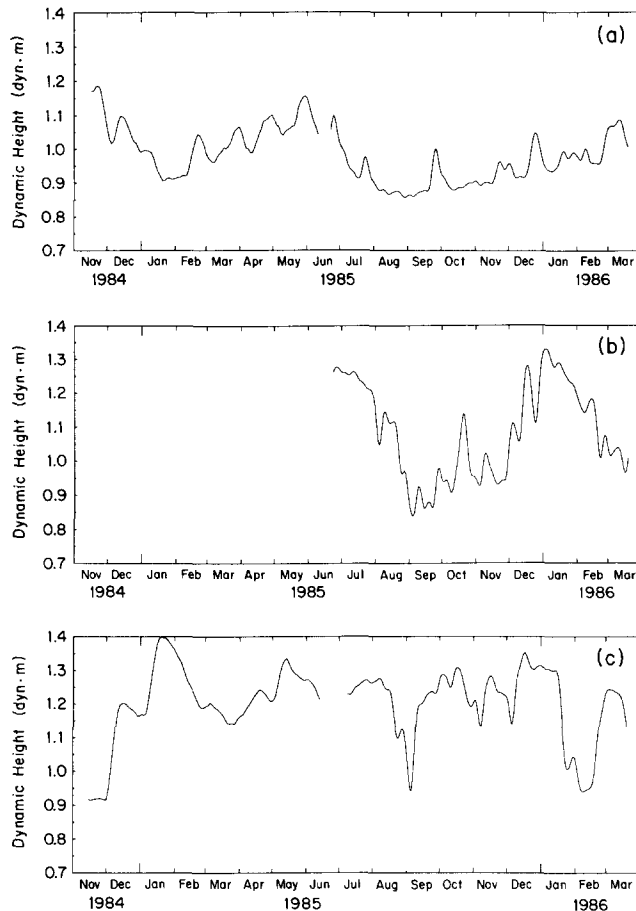


Fig. 9. Time series of dynamic height for the three locations during the total observed period. Data have been smoothed by a 10-day running mean of the original values. (a) Western location, IES Sta. 3 ( $37^{\circ}29'S$ ,  $53^{\circ}49'W$ ). (b) Intermediate location, IES Sta. 2 ( $37^{\circ}47'S$ ,  $52^{\circ}46'W$ ). (c) Eastern location, IES Sta. 1 ( $37^{\circ}58'S$ ,  $51^{\circ}56'W$ ).

west displacement of the front: during November 1984 the front travels 70 km to the east ( $X = 70-0$  km), on 20 May it moves 50 km toward the west. From 28 May to 5 August the front moves 150 km toward the east at an average speed of  $2.2 \text{ km day}^{-1}$  ( $2.5 \text{ cm s}^{-1}$ ). On 28 December 1985, the front starts a fast westward motion ( $14.4 \text{ km day}^{-1}$  or  $16.7 \text{ cm s}^{-1}$ ) toward  $X = 40$  km. This suggests a 6-month oscillation superimposed on the main displacement of the front that has a time scale of 12 months during the observed period.

The above-described 6-month oscillation also can be observed in the time series of dynamic height: in Fig. 8a from November 1984 to June 1985 (front at IES Sta. 1) and in Fig. 8b from June 1985 to January 1986 (front at IES Sta. 2). A visual overlap of these two segments of the figures shows two complete cycles within 6 months.

Analysis of the time series of dynamic height at the three locations (Fig. 9) allowed us to decide on the ambiguity of the position of the front for February and March 1986. In

February 1986 (Fig. 9c), and at the end of March 1986 (Fig. 2c), a cold intrusion is observed at  $51^{\circ}56'W$ . This is also observed further west ( $52^{\circ}45'W$ ) during March 1986. Minimum values of dynamic height are observed in all three cases. That is to say that this period of time is characterized by multiple cold intrusions formed or in the process of being formed east of the location of the confluence zone. That the front is located near  $X = 0$  km for the period February and March 1986 is confirmed by infra-red satellite images (e.g. Fig. 10).

One possible explanation for the low-frequency motion of the front is the variability in the northward penetration of the Malvinas Current. If the current extends further north (north of  $38^{\circ}S$ ), this would result in an eastward displacement of the warm waters of the Brazil Current, while if the northern extent of the Malvinas Current moves to the south, the front will be located further west. This motion, at least for the monitored period, seems to have a time scale of 12 months.

Superimposed to the 6/12-month period variability there are other oscillations present in the two records (Fig. 8a,b). The dynamic height time series show oscillations with periods of 20–30 days. This is reflected in the time series obtained for the frontal position. It is interesting to note that this oscillation appears only at the location of the front. If the front is displaced more than 100 km to the east (Fig. 8a, August to November 1985), only an oscillation of about 2 months remains. On the basis of infra-red satellite images, LEGECKIS and GORDON (1982) showed that the southward limit of the Brazil Current had a meridional fluctuation with a period of about 2 months. The oscillations observed in the time series somehow could be related to this fluctuation. A more extensive (north–south) array of instruments would be necessary to determine the characteristics of this motion.

#### *Offshore eddies and intrusions*

The time series of dynamic height at the offshore location (Fig. 9c) is characterized by a generally constant value ( $\approx 1.25$  dyn m) and sporadic large departures or anomalies that have durations of about 1 month: three intense cold anomalies ( $\Delta D \approx 0.3$  dyn m), and one warm anomaly ( $\Delta D \approx 0.2$  dyn m) are observed.

The cold and warm intrusions observed from November 1984 to June 1985 were described by GARZOLI and BIANCHI (1987). It was concluded that the cold anomaly during November–December 1984 corresponds to a cold intrusion associated with cyclonic motion. The increase in dynamic height observed during January 1985, at the offshore location (IES 1, Fig. 1, Fig. 9c), corresponds to a southern entrainment of the warm waters associated to the Brazil Current.

In September 1985, a cold anomaly in dynamic height is observed at the offshore location (IES 1, Fig. 9c) that is present in the record for about 20 days and that might be associated with a cold cyclonic eddy. However, the geostrophic velocity between the two easternmost stations (Fig. 7c) does not show a northward flow during that period of time. This contradiction can be explained by considering that according to Fig. 8b, the cooling at the offshore location occurs simultaneously with a more intense cooling at the intermediate location (IES 2, Fig. 8b); the front is located east of IES 2 (Fig. 4). Therefore, it can be assumed that the cyclonic motion that should be associated with this cold anomaly is masked by the strong resultant flow due to both the Brazil Current and the Malvinas return and cannot be resolved in this spatial scale.

Another cold anomaly is observed during January and February 1986. That it corresponds to a cyclonic motion associated with a cold eddy can be concluded from the

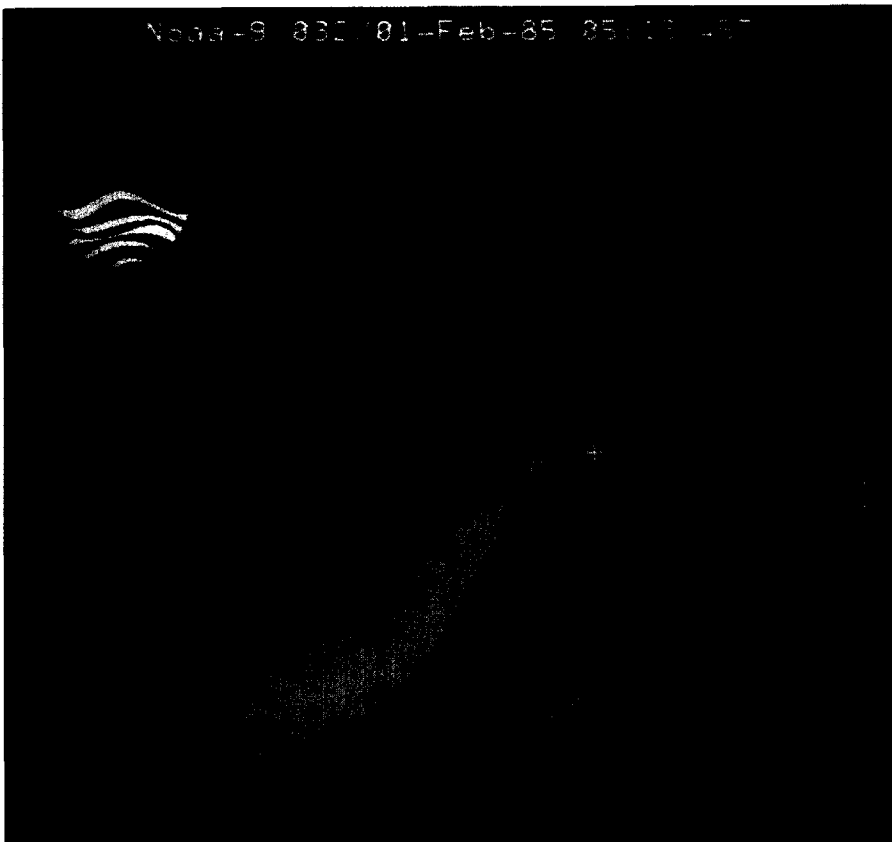


Fig. 10. A sample of NOAA AVHRR satellite image obtained for 1 February 1986. Red and yellow colors are warm temperature characteristics of the Brazil Current. Blue and green colors are temperature characteristics of the Malvinas Current (BROWN and EVANS, personal communication). The + show the positions of three inverted echo sounders discussed in this study.

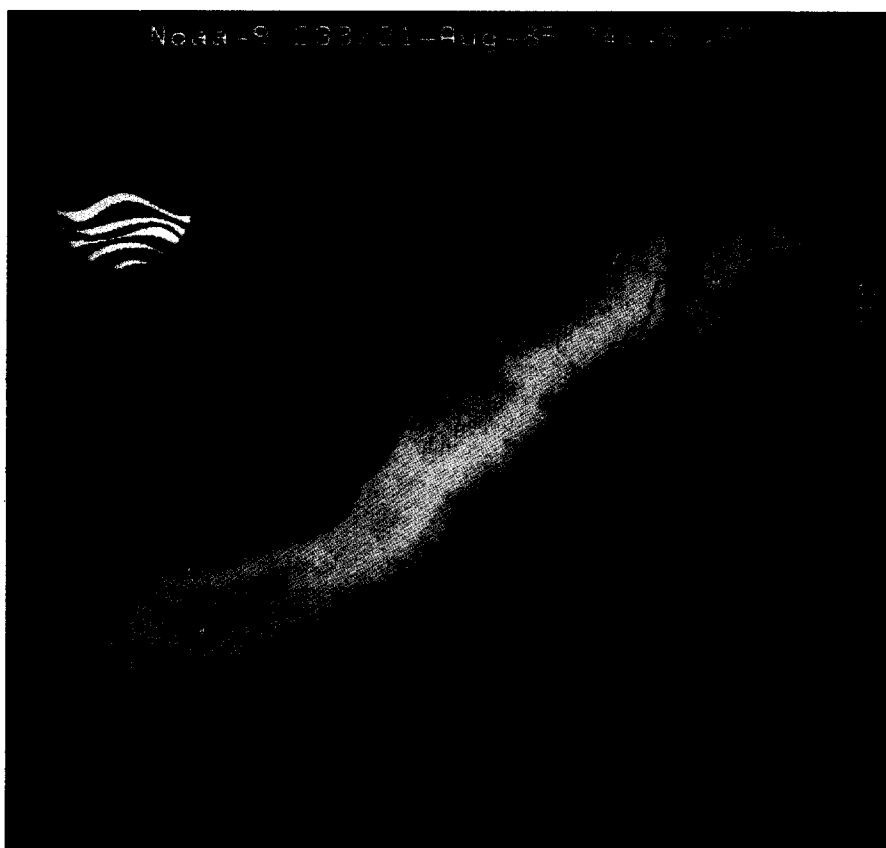


Fig. 11. Same as Fig. 10 for 21 August, 1985. Here the Brazil Current is represented by yellow and green colors while different tones of blue are related to the Malvinas water.

analysis of the geostrophic velocities (Fig. 7c). The surface velocity associated with the eddy is of  $\approx 30 \text{ cm s}^{-1}$  toward the north. Shortly after this anomaly is no longer detected at the offshore location, on 1 March 1986 a new one begins to be formed (see Fig. 2; due to the smoothing of the data, only the beginning of the formation can be observed on Figs 7 and 8). A value for the anomaly in dynamic height of 0.3 dyn m is obtained, and the associated surface velocity is  $20 \text{ cm s}^{-1}$ .

Therefore, during the 17-month monitored period, cold intrusions with cyclonic motions associated with cold eddies are observed with no apparent periodicity. The surface velocities range from 20 to  $30 \text{ cm s}^{-1}$  and the duration in the records from 20 to 60 days.

The available potential energy associated with these eddies can be estimated from hydrographic data. The available potential energy of a cold eddy immersed in warm water is given by

$$\text{APE} = \rho g' \int 2\pi r \, dr (h(r) - h_0)^2, \quad (5)$$

where  $r$  is the radial coordinate,  $h$  is the depth of the thermocline, and  $h_0$  is the depth away from the eddy influence area. From the hydrographic data, a value for the reduced gravity was obtained ( $g' = 0.013 \text{ m s}^{-2}$ ), and it was assumed that the depth of the  $8^\circ\text{C}$  isotherm is representative of the thermocline in the area. The hydrographic observations obtained during October 1984 were used to calculate the APE of an eddy of cylindrical shape. The function  $h(r)$  was obtained from hydrographic data. The value obtained for  $h_0$  is  $h_0 = 450 \text{ m}$ . The resulting value for the APE according to equation (5) is  $6.5 \times 10^{15} \text{ J}$ . This value is of the same order of magnitude as values obtained for Gulf Stream eddies.

## 5. CONCLUSIONS

The foregoing analysis demonstrates that through a combination of inverted echo sounders and hydrographic data the study of a region as complex as the South Atlantic Confluence is feasible. Data have been calibrated to absolute dynamic height with an error of  $\pm 0.03 \text{ dyn m}$ , which represents 2.5% of the main detected signals. Relative geostrophic velocities are obtained from the dynamic height time series with an error from  $\pm 1.35$  to  $2.25 \text{ cm s}^{-1}$ . The position of the strong subsurface thermal front is determined with an error ranging from 4 to 15 km.

During the monitored period (Fig. 7c), the geostrophic velocity from the surface relative to 800 m reaches a maximum value of  $55 \text{ cm s}^{-1}$  ( $\pm 2.20 \text{ cm s}^{-1}$ ) in September–October 1985. From this calculation the associated transport relative to 800 m is 18 Sv, which represents an approximate transport of 22 Sv relative to 1400 m. This value corresponds to a situation in which the Malvinas Current has penetrated further north; the observed flow could be the result of a composite of the Brazil Current and the Malvinas return.

It is also possible, from the dynamic height time series, to obtain an estimation for the related transports of the meridional currents near the confluence region. The mean surface geostrophic velocity associated with the Brazil Current is  $35 \text{ cm s}^{-1}$  ( $\pm 2.2 \text{ cm s}^{-1}$ ), and the mean estimated transport 11 Sv relative to 800 m. This is in good agreement with the value for the Brazil transport obtained from hydrography (Table 2) and with those obtained previously by GORDON and GREENGROVE (1986). The mean geostrophic surface velocity relative to 800 m associated to the Malvinas Current return flow at the vicinity of the front is  $9 \pm 2 \text{ cm s}^{-1}$  and the transport 3.5 Sv.

Four cold intrusions are detected, with no apparent periodicity in the 17-month record obtained at the offshore location. Three of them are associated with cold cyclonic eddies with a surface shear of about 20 to 30 cm s<sup>-1</sup>; they are present in the records for periods of time that range from 20 to 60 days. The available potential energy associated with these cyclonic motions is  $6.5 \times 10^{15}$  J.

The simultaneous analysis of the dynamic height time series (or depth of the thermocline) and location of the front (or distance to the inshore sounder) indicates that the main motion observed during the 17-month period of measurements in the convergence of the Brazil and Malvinas currents is a low-frequency east–west displacement of the front: from November 1984 to June 1985 the front is located near 54°W. This situation corresponds to a southern latitude of separation for the Brazil Current and a consequent southern latitude for the maximum intrusion of the Malvinas Current. In June 1985, the separation occurs further north (northward penetration of the Malvinas Current) originating a displacement of the front toward the east at about 53°W. Six months afterward the front returns to its original location (54°W). These results are confirmed by infra-red satellite images (Figs 10 and 11; OLSON *et al.*, 1988). During August, the Malvinas Current penetrates up to 33°S (Fig. 11) and the front is located at IES Sta. 2. In February (Fig. 10), the northward extension of the Malvinas Current is further south and the thermal front can be observed at IES Sta. 3. Therefore, it is concluded that there is a low frequency east–west motion of the front with a period close to 1 year and related to the variability in the latitude of separation of the Brazil Current. Superimposed to the above-described east–west displacement, the front undergoes oscillations with periods of 1–2 months. They are possibly related to instabilities of the front and/or to a north–south motion of the southern boundary of the Brazil Current at a constant latitude of separation as described by LEGECKIS and GORDON (1982).

One of the factors that determines the separation of a boundary current like the Brazil Current is the increase of the Coriolis parameter with latitude (CHARNEY, 1955; OU and DE RUIJTER, 1986). The previously discussed observations indicate an 11- to 12-month period of variability in this separation latitude directly associated with a northward penetration of the Malvinas Current. Also, recent theoretical results (PHILANDER and PACANOWSKI, 1987) and observations (RICHARDSON and REVERDIN, 1987) of the equatorial Atlantic suggest a seasonal variability in the intensity of the Brazil Current. Does the Malvinas Current extend further north because the latitude of separation occurs earlier (due to a weaker southward flow)? Or does a stronger Malvinas Current cause a northward separation of the Brazil Current? To answer this question, extended field work and numerical modeling is necessary. An effort in this direction will be started by the time this paper is published. Until then, a plausible explanation is that there is variability in the intensity of the Malvinas Current due to the variability of the winds in the South Atlantic (south of 45°S) which produce the observed changes in the latitude of separation.

*Acknowledgements*—Drs A. Gordon and D. Olson provided useful comments while reviewing the original manuscript for which we are grateful. Electronic engineers in charge of the instruments were E. Draganovic and Miguel Macció. Sarah Rennie and Mark Edwards have performed the computer programming necessary for the data reduction and analysis. Susan Brower typed the manuscript. The inverted echo sounders were deployed and recovered by the Argentine R.V. *Oca Balda*. Silvia Garzoli is indebted to the authorities of Instituto Nacional de Investigación y Desarrollo Pesquero (INIDEP) for the use of the ship; all members of the crew for their collaboration during the cruise; to the Consejo Nacional de Investigaciones Científicas y Técnicas

(CONICET) and Servicio de Hidrografía Naval (SHN) for their support in the local organization and realization of the cruises. This program has been supported by grants from the Office of Naval Research, contract N00014-84-0132 and N00014-87-K-0204 as part of their Southern Ocean Accelerated Research Initiative. Z. Garraffo's participation on the data analysis was jointly supported by CONICET and a grant from the Tinker Foundation, LDGO contract CU00327801. This is LDGO contribution no. 4447.

## REFERENCES

- BROWN O. B., D. B. OLSON and R. H. EVANS (1986) Brazil Current Confluence variability. Abstract from the Mar del Plata, Argentina Meeting, March.
- CAMP D., W. HAINES and B. HUBER (1985) Marathon Leg 7 R/V *Thomas Washington* CTD/Hydrographic Data. Preliminary Report. Lamont-Doherty Geological Observatory.
- CHARNEY J. G. (1955) The Gulf Stream as an inertial boundary layer. *Proceedings of the National Academy of Science, U.S.A.*, **41**, 731–740.
- GARZOLI S. L. and M. E. CLEMENTS (1986) Indirect wind observations in the southwestern Atlantic. *Journal of Geophysical Research*, **91**, 10,551–10,556.
- GARZOLI S. L. and A. BIANCHI (1987) Time-space variability of the local dynamics of the Malvinas–Brazil Confluence as revealed by inverted echo sounders. *Journal of Geophysical Research*, **92**, 1914–1922.
- GORDON A. L. (1989) Brazil–Malvinas Confluence—1984. *Deep-Sea Research*, **36**, 359–384.
- GORDON A. L. and C. L. GREENGROVE (1986) Geostrophic circulation of the Brazil–Falkland Confluence. *Deep-Sea Research*, **33**, 573–585.
- GUERRERO R. A., A. A. BIANCHI and A. R. PIOLA (1986) Datos Físico Químicos, CTD Y XBT. Puerto Deseado, Campaña 02/1984. Oca Balda, Campaña 04/1985. Servicio de Hidrografía Naval, Departamento Oceanografía, Informe técnico No. 39, 114 pp.
- GUERRERO R. A., A. A. BIANCHI and A. R. PIOLA (1987) Datos Físico Químicos, CTD Y XBT. Oca Balda, Campaña 02/1986. Servicio de Hidrografía Naval, Departamento Oceanografía, Informe técnico No. 40, 45 pp.
- LEGECKIS R. and A. L. GORDON (1982) Satellite observations of the Brazil and Falkland Currents 1975 to 1976 and 1978. *Deep-Sea Research*, **29**, 375–401.
- OLSON D. B., S. EMERSON, M. CARLE, O. B. BROWN and R. EVANS (1986) Large-scale surface circulation in the South Atlantic from satellite IR and drifter data. Abstract from Mar del Plata, Argentina Meeting, March.
- OLSON D. B., G. P. PODESTA, R. H. EVANS and O. B. BROWN (1988) Temporal variations in the separation of Brazil and Malvinas Currents. *Deep-Sea Research*, **35**, 1971–1990.
- OU H. W. and W. P. M DE RUIJTER (1986) Separation of an inertial boundary current from a curved coastline. *Journal of Physical Oceanography*, **16**, 280–289.
- PHILANDER S. G. H. and R. PACANOWSKI (1987) The mass and heat budget in a model of the tropical Atlantic Ocean. *Journal of Geophysical Research*, **91**, 14212–14220.
- RICHARDSON P. and G. REVERDIN (1987) Seasonal cycle of velocity in the Atlantic North Equatorial Countercurrent as measured by surface drifters, current meters and ship drift. *Journal of Geophysical Research*, **92**, 3691–3708.
- RODEN G. I. (1986) Thermohaline fronts and baroclinic flow in the Argentine Base during the austral spring of 1984. *Journal of Geophysical Research*, **91**, 5075–5093.
- RODEN G. I. and W. J. FREDERICKS (1986) Southwest Atlantic Ocean Marathon Expedition, Leg 8. R/V *Thomas Washington* 26 October–17 November 1984. Data Report. University of Washington.
- WATTS D. R. and H. T. ROSSBY (1977) Measuring dynamic heights with inverted echo sounders: results from MODE. *Journal of Physical Oceanography*, **7**, 345–358.